

Veröffentlichung

Im Rahmen des SFB 880. www.sfb880.tu-braunschweig.de

Autoren

Burnazzi, Marco;Radespiel, Rolf

Titel

Synergies between suction and blowing for active high-lift flaps

Publisher o. Konferenz

CEAS Aeronaut Journal, DOI 10.1007/s13272-014-0146-8

Jahr

2014

Internet-Link (Doi-Nr.)

<http://link.springer.com/article/10.1007%2Fs13272-014-0146-8>

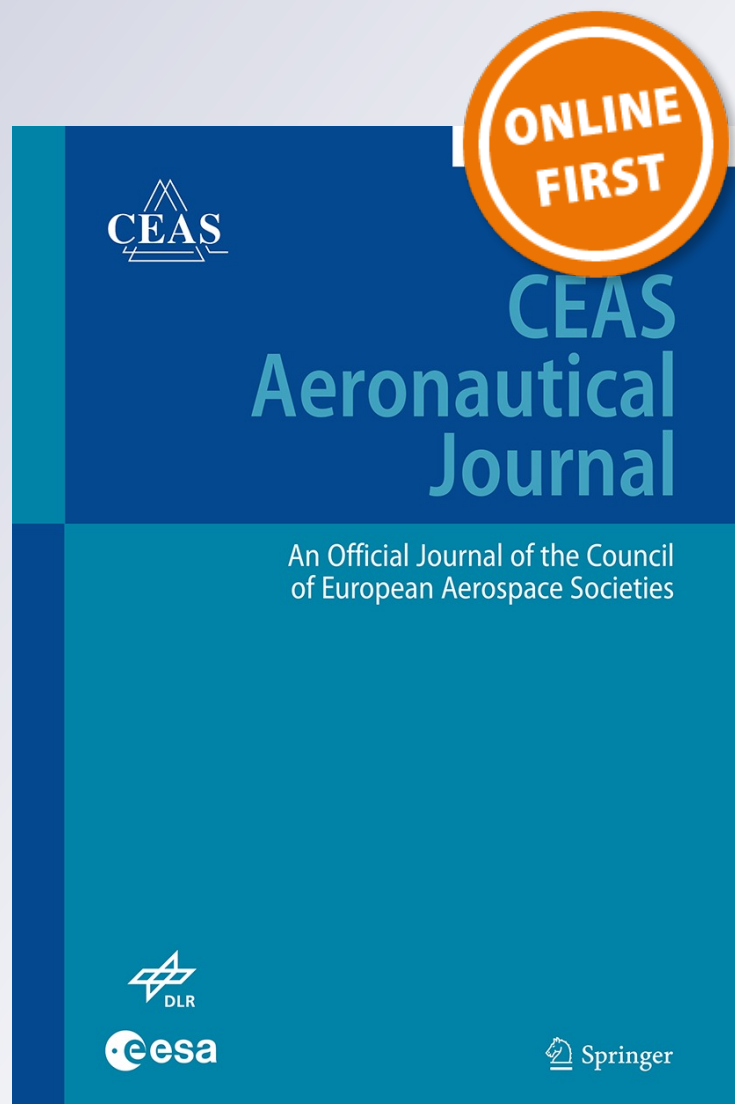
Synergies between suction and blowing for active high-lift flaps

M. Burnazzi & R. Radespiel

CEAS Aeronautical Journal
An Official Journal of the Council of
European Aerospace Societies

ISSN 1869-5582

CEAS Aeronaut J
DOI 10.1007/s13272-014-0146-8



Your article is protected by copyright and all rights are held exclusively by Deutsches Zentrum für Luft- und Raumfahrt e.V.. This e-offprint is for personal use only and shall not be self-archived in electronic repositories. If you wish to self-archive your article, please use the accepted manuscript version for posting on your own website. You may further deposit the accepted manuscript version in any repository, provided it is only made publicly available 12 months after official publication or later and provided acknowledgement is given to the original source of publication and a link is inserted to the published article on Springer's website. The link must be accompanied by the following text: "The final publication is available at link.springer.com".

Synergies between suction and blowing for active high-lift flaps

M. Burnazzi · R. Radespiel

Received: 9 January 2014 / Revised: 8 December 2014 / Accepted: 18 December 2014
© Deutsches Zentrum für Luft- und Raumfahrt e.V. 2015

Abstract The present 2-D CFD study investigates aerodynamic means for improving the power efficiency of an active high-lift system for commercial aircraft. The high-lift configuration consists of a simple-hinged active Coanda flap, a suction slot, and a flexible droop nose device. The power required to implement circulation control is provided by electrically driven compact compressors positioned along the wing behind the wingbox. The compact compressors receive air from the suction slot, which also represents an opportunity to increase the aerodynamic performance of the airfoil. The present work investigates the aerodynamic sensitivities of shape and location of the suction slot in relation to the maximum lift performance of the airfoil. The main purpose of the study is the reduction of the compressor power required to achieve a target lift coefficient. The compressor power requirements can be reduced in two ways: obtaining a high total pressure at the end of the suction duct (compressor inlet) and reducing the momentum needed by the Coanda jet to avoid flow separation from the flap. These two objectives define the guideline of the suction slot design. As a result, a jet momentum reduction of 16 % was achieved for a target lift coefficient of 5 with respect to the same configuration without suction. Furthermore, the study yielded physical insight into the aerodynamic interaction between the two active flow control devices.

Keywords Flow control · Coanda flap · Wall suction · Active high-lift

List of symbols

C_μ	Momentum coefficient of the Coanda jet
v_J	Coanda jet velocity
\dot{m}_J	Coanda jet mass flow
v_∞	Freestream velocity
ρ_∞	Freestream density
S_{ref}	Reference surface
M	Mach number
Re	Reynolds number
α	Angle of attack
P_{ti}	Total pressure at the end of the suction duct
M_{inlet}	Mach number at the end of the suction duct
$C_{l,\text{max,bal}}$	Balanced maximum lift coefficient
$C_{\mu,\text{bal}}$	Balanced jet momentum coefficient
δ_2	Boundary layer momentum thickness
c	Airfoil chord length
δ	Flap deflection angle
γ	Diffuser angle
β	Local duct-to-wall angle
x	Suction slot location

1 Introduction

Active flow control is a promising solution to reduce aviation's rising problems related to noise emissions, fuel consumption and traffic congestion. The efficacy of controlling the behavior of the flow around an object by actively altering the boundary layer momentum was demonstrated by Prandtl [1] in 1927. Since then, a large variety of flow control techniques has been developed assessing the potential of active circulation control for improving the

This paper is based on a presentation at the German Aerospace Congress, September 10–12, 2013, Stuttgart, Germany.

M. Burnazzi (✉) · R. Radespiel
Institute of Fluid Mechanics, Technische Universität
Braunschweig, Hermann-Blenk-Str. 37,
38108 Braunschweig, Germany
e-mail: m.burnazzi@tu-bs.de

aerodynamic performances of wing airfoils. However, the integration of the active system into the aircraft is still a major problem. This is mostly related to the limited availability of power needed to implement circulation control. For this reason, the reduction of the power required to obtain a target lift and the definition of alternative power sources are the main challenges of the current research on active high-lift systems. In this context, the present work contributes to the development of an active high-lift configuration, focusing on the aerodynamic efficiency to reduce power requirements.

The active high-lift configuration investigated here is based on a Coanda flap. A thin air jet is tangentially blown over the suction side of a deflected simple-hinged flap to avoid flow separation from the flap surface. This device significantly increases the circulation around the airfoil, creating the need of a leading-edge device to reduce the suction peak at the leading edge and increase the stall angle of attack. For this purpose the leading edge of the current configuration is equipped with a flexible droop nose device. The compressed air required for the Coanda jet is provided by a set of compact electric compressors integrated into the wing near the flap [2], as shown in Fig. 1. The present paper focuses on the design of the air intake of the compact compressors, since a suction slot positioned on a convenient location on the airfoil can contribute to the aerodynamic efficiency of the high-lift system. In particular the following objectives define the guideline of the design process:

- High-lift coefficients and high angles of attack at maximum lift.
- High total pressure recovery at the end of the suction duct.

Location and geometry of the blowing device are kept fixed during the analyses presented here. The main purpose

of the study is the assessment of the combination of the two flow control techniques, blowing and suction, for the reduction of the momentum required by the Coanda jet to meet a certain lift target. The study shows that a positive interaction between the two devices is obtained by positioning the suction slot on the suction side of the airfoil upstream of the blowing device. The consequent reduction of boundary layer thickness on the suction side of the airfoil significantly reduces the jet momentum required to avoid flow separation from the flap. This configuration yields a reduction of 16 % of the jet momentum needed to reach a target lift coefficient of 5, with respect to the same configuration without suction. Locating the suction slot on the flap surface or on the pressure side of the airfoil results in higher jet momentum requirements.

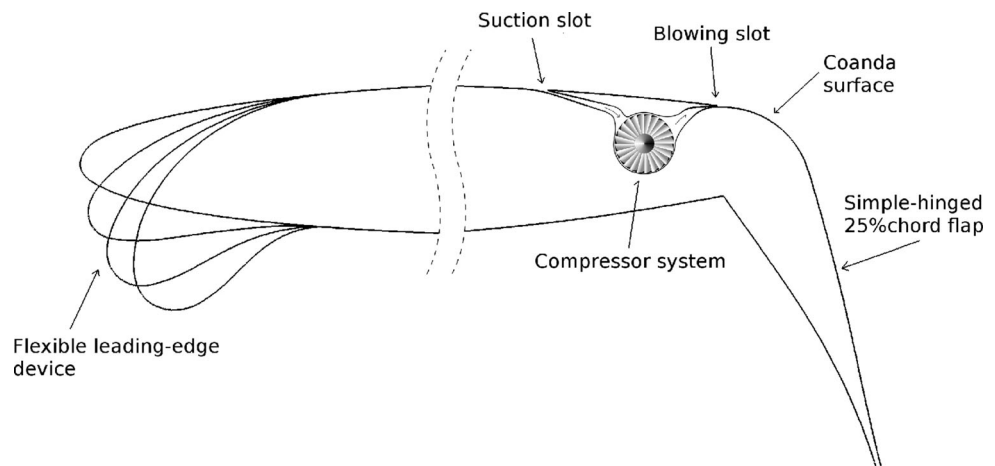
1.1 Background

As transportation plays a primary role in global economic development, there is a need to assure efficient world-wide mobility. The current growth of the Asian market and the global urbanization, for example, drive projections of a strong expansion of the world traffic volume in the next decades. The NASA blueprint for aeronautics [3], released in August 2013, identified the following drivers to be strategic for future aviation research programs:

- Global growth in demand for air mobility.
- Climate issues, sustainability, energy transition.
- Technological exchange among different fields.

Defined by these drivers, the long-term vision for sustained air transportation aims at improving the quality of the commercial service and solving issues arisen from the continuous increase of passengers and goods transport of the last decades. The reductions of fuel consumption and travel time are among the main objectives. An effective

Fig. 1 Scheme of the high-lift configuration



solution to these problems is to extend the commercial transport to small airports, currently unused in this respect. Enabling aircraft to perform point-to-point connections would also relieve the congestion at the big hub airports, which has been causing frequent flight delays in the last years. In order to access smaller airports, a new class of aircraft will have to operate from short runways and have low noise emissions. In this context, a technological challenge is represented by the high-lift systems. Innovative solutions should yield significant flight speed reductions at takeoff and landing, and reduced airframe noise in these conditions. Both objectives, high-lift coefficients and reduced noise emissions, can be successfully addressed by exploiting the potentials of active circulation control.

The active control of boundary layer separation makes it possible to obtain high-lift targets without employing gaps, which were identified as a major source of noise generated by conventional high-lift devices [4]. However, introducing active high-lift devices into commercial aviation raises many technological issues, mostly related to the source of power required by the active high-lift system. Preliminary design of cruise efficient aircraft states that substantial reductions of runway length are only possible by increasing the maximum lift coefficient by significant factors accompanied with a moderate increase of the installed engine thrust [5]. For this reason, the current technological challenge is the reduction of power requirements through a significant improvement of the aerodynamic efficiency of the circulation control.

A thorough overview on the existing studies concerning boundary layer control applications, for several body shapes and control principles, is given by Wygnanski [6]. Gad El Hak [7] categorized the various control schemes in flow control based on energy expenditure. He recognized direct tangential injection of momentum into the boundary layer—wall jet—as one of the most effective and feasible flow separation control techniques. Englar [8] discussed several applications of this principle, showing the potential of tangential blowing for lift generation or drag reduction in a large variety of fields, including aircraft, cars and trucks. A major advantage of a wing equipped with an active circulation control system is the possibility to enhance lift generation with a substantial simplification of the mechanical apparatus. Blowing over a blunt trailing edge, for instance, modifies the Kutta condition and allows control of the rear stagnation point without employing mechanical devices. However, a wide blunt trailing edge needs active blowing also during cruise phases, since a wide recirculation region at the trailing edge would cause high form drag. For this reason, it is more convenient to employ a mechanical flap equipped with a tangential wall jet to enable flow attachment even at high deflection angles. This configuration has the potential to achieve a

high flow curvature with a simple mechanical mechanism and the advantage of not affecting the cruise performance. This approach has been the interest of several research programs, including the present one. Milholen et al. [9] published experimental results from the NASA-LaRC National Transonic Facility, where high Reynolds number tests were conducted on the “FAST-MAC” model, a tapered, swept and twisted supercritical wing model equipped with an active circulation control flap. A wall jet was blown tangentially on the suction side of the 15 % chord simple-hinged flap, deflected by 60° in landing configuration. The experiments showed that the circulation control improved the low-speed maximum lift coefficient by 33 %.

Another way to prevent flow separation by modifying the natural behavior of the flow near the wall is the suction of a portion of the boundary layer through a suction slot. This principle was first explored by Prandtl in 1904. He applied suction to one side of a circular cylinder by means of a narrow slit. As the slit was positioned about 10° downstream of the original separation point, separation was delayed on that side of the cylinder. As a result the drag was greatly reduced, and a transverse force was produced. According to Schlichting [10], the effect of boundary layer suction is essentially based on a change of the velocity outside of the boundary layer. The conventional velocity field is superimposed to the sink velocity distribution generated by the wall suction. This results in an accelerated flow upstream of the sink, thus preventing separation. Downstream of the suction slit the outer flow is decelerated, but now the boundary layer is thinner and can therefore withstand greater adverse pressure gradient without separation. Different suction-slot shapes were investigated by Loftin [11] with the purpose of extending the area of laminar boundary layer to reduce drag. According to Loftin's study, a wide suction slot reduces the total pressure loss inside the duct, but creates a disturbance in the boundary layer of the external flow. Chen et al. [12] tested the behavior of boundary layer suction on a thick airfoil to control trailing edge separation, and compared the lift performance with a blowing device applied on the same airfoil. For a low momentum of the flow through the slot, suction provided higher lift, whereas blowing was more effective with a higher momentum. The location and width of the blowing/suction slot were also investigated. Suction was more effective with a wide slot located downstream of the natural separation line, whereas blowing was improved by a narrow slot positioned upstream of the natural separation line.

From the large number of published studies addressing active flow control, it is clear that an extremely careful design of the flow control system is essential for its efficiency. Several parameters should be investigated to assess the potential of a particular flow control mechanism. Slot

thickness and location, for instance, may have different optimal values for various airfoil geometries or flow conditions. For this reason it is necessary to create a comprehensive database of the aerodynamic sensitivities of the parameters involved in the design process. In this context computational fluid dynamics (CFD) is an extremely powerful tool. However, active control represents a challenge for the accuracy of numerical solutions. Allan et al. [13] and Paschal et al. [14] performed 2D numerical and experimental analyses on a circulation control airfoil characterized by a large circular trailing edge, over which a wall jet was blown. The thick trailing edge allowed accurate pressure measurements and offered a large Coanda surface where the accuracy of the numerical approach could be tested for different blowing rates. In the absence of a separation point fixed by a sharp edge, the Kutta condition depended entirely on the jet momentum. In this condition the solution of a numerical simulation is particularly sensitive to the capability of the turbulence model to accurately estimate the eddy viscosity, even in the presence of high flow curvature.

An important requirement for transport aircraft applications calls for low actuation power of the active control system, as otherwise a significant engine growth will occur. The efficiency of active blowing is usually characterized by the lift gain factor, defined as the ratio between the increase of lift coefficient due to the active circulation control system and the jet momentum coefficient needed to obtain this gain. The lift increase is with respect to the maximum lift coefficient of the airfoil in cruise configuration. In the present study, the cruise C_l was numerically determined for the airfoil shown in Fig. 2, $C_{l,max} = 1.87$, for a chord Reynolds number of 12×10^6 . The jet momentum coefficient is given by:

$$C_{\mu} = \frac{v_J \dot{m}_J}{\frac{1}{2} \rho_{\infty} v_{\infty}^2 S_{ref}}$$

where v_J and \dot{m}_J are the velocity and the mass flow of the jet at the exit section of the plenum. Quantitative values of lift gain factor had not previously received much attention. Recently, Radespiel et al. [15] reviewed the status of published lift gain factors, where the detailed design of blowing slot height, flap angle and Coanda contour along

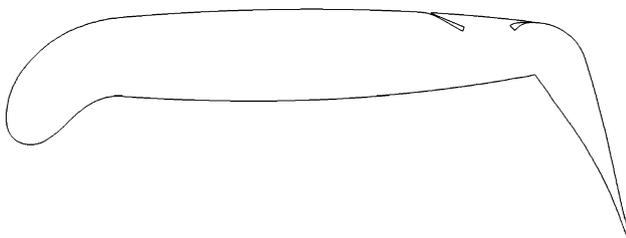


Fig. 2 Analyzed high-lift configuration

with the blowing rate was found to have a significant impact on the gain factor. Improvements in gain factor can be obtained by numerical sensitivity investigations to guide the design. Recent design data reveal that lift gain factors of 80 are obtained for active airfoils with maximum lift coefficients of 4 when using steady blowing [16–18]. Note that the gain factor decreases rapidly towards higher lift coefficients. Also, significantly reduced angles of attack for maximum lift are observed at high flap angles and high blowing. It turns out that the suction peak near the airfoil leading edge generated by the active high-lift flap is responsible for these behaviors. This calls for aerodynamic means to reduce the losses associated with the flow around the leading edge. The solution adopted within the framework of the present project is a carefully designed droop nose. This device, associated with an active Coanda flap, provides a significantly higher effect than when employed together with a conventional fowler flap [19, 20]. These findings represent the starting point of the present paper.

1.2 Paper outline

Sections 2 and 3 describe the employed high-lift configuration and the numerical approach used for the analysis. Section 4 presents the sensitivity study of different suction slot geometrical parameters, which explains the physical principle of the wall suction and the resulting increase of performance. Subsequently, the response to different jet momentum coefficients is presented in Sect. 5. Here wall suction is also applied to the clean nose configuration, showing the larger benefit generated by the new device in combination with the droop nose. Finally, the results of the previous analyses are summarized by comparing the jet momentum needed by the different configurations to reach a lift coefficient of 5 at the angle of maximum lift. The wall suction yields a reduction of 16 % of the required jet momentum with respect to the same configuration without suction. In the same condition the stall angle of attack is increased by 3° and the pitching moment coefficient reduced by 11 %.

2 High-lift configuration

The DLR F15 airfoil in high-lift configuration, analyzed in the present work, is shown in Fig. 2. The high-lift configuration consists of three devices:

- Coanda trailing edge flap.
- Droop nose leading edge.
- Suction slot.

The present study deals with the implementation of the suction slot on the previously designed configuration. Thus, Sects. 2.1 and 2.2 describe the starting point of the work.

2.1 Trailing edge device

This section summarizes our previous numerical and experimental investigations aimed at improving the lift gain factor by careful adjustments of the trailing edge design parameters, while the leading edge was geometrically fixed. These initial design studies assumed steady blowing tangential to the flap surface to produce suited turbulent wall jets that exploit the Coanda effect for effective flow turning. The results indicated that the most important design parameters are the flap deflection angle, the blowing momentum coefficient, and the blowing slot height [16]. Whereas flap angle and blowing momentum coefficient should increase for increased lift targets, slot heights remain rather small, with values of around 0.0006 times the airfoil chord length. Surprisingly, the optimum slot height was found independent of the flap angle. The detailed curvature distribution of the Coanda surface used as flap knuckle shape was found to be less important. The internal shape of the duct was designed with the upper and lower walls parallel to each other at the exit section. A contraction rate of 15 was employed to obtain a realistic jet velocity profile.

Figures 3 and 4 illustrate a typical design result, where the transonic airfoil DLR F15 is equipped with an internally blown flap set at 65° deflection angle.

Values of the radius of curvature of 0.07 times the chord length were a reasonable design choice. The flap length suited to achieve high-lift gains was also identified, with the best lift gain factors obtained with flap lengths of 0.25–0.30 times the airfoil chord [16]. With these design choices and assuming steady wall jet blowing, typical lift gain factors of ~80 were obtained at a lift coefficient around 4 and with a flap deflection angle of 50°. The lift

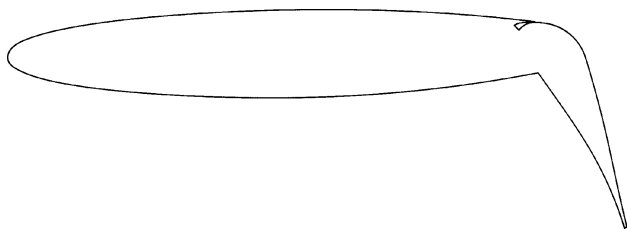


Fig. 3 DLR F15 airfoil, equipped with an active Coanda flap

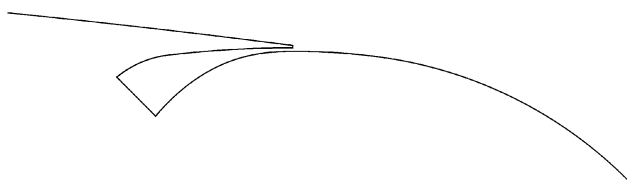


Fig. 4 A close-up of the blowing slot

gain factor was reduced to 55 at a lift coefficient about 6 and $\delta = 80^\circ$. The flap deflection employed in the present study, $\delta = 65^\circ$, yields a lift gain factor of 72 at $C_l = 4.38$.

Figure 5 shows the reduction in the angle of attack of maximum lift with higher blowing rates. As the adverse pressure gradient along the suction side grows rapidly with the angle of attack it creates significant momentum losses towards the trailing edge device. These momentum losses adversely affect the ability of the wall jet to provide flow turning. Local blowing at the nose or at other locations of the airfoil did not help much, as it extended the useful angle-of-attack range but generally at the cost of decreasing the lift gain factor [17, 21]. It is worth to note that the simulations predicted leading edge stall for the DLR F15 airfoil at lift coefficients above 6.

2.2 Leading-edge device

The high circulation generated by the active flap dramatically reduces the stall angle of attack. This is due to the high curvature of the streamlines at the leading edge. With an increase of lift, the stagnation point moves downstream along the pressure side, accelerating the flow around the leading edge. Conventional high-lift systems employ slotted leading-edge devices, slats, to address this problem. However, one of the main objectives of the present work is the noise reduction, which is pursued by avoiding the use of gaps. Following this guideline a flexible gap-less leading-edge device was developed [19]. Details on the performances of the leading-edge device, as well as a comparison with a conventional slat configuration, are discussed by Burnazzi and Radespiel in [22]. As illustrated in Fig. 2, the camber line and the thickness are increased, resulting in a reduction of the suction peak at the leading edge. The morphed shape makes it possible to distribute the low pressure area on a wider surface, reducing the

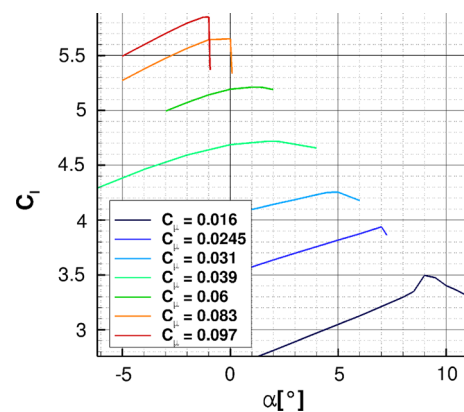


Fig. 5 Effect of blowing momentum on the angle of maximum lift for the DLR F15 airfoil with 65° flap angle, computed for $M = 0.15$, $Re = 12 \times 10^6$

minimum pressure values. This new load distribution results in different stall behaviors [22]. Figure 6 shows a comparison between the clean nose and the droop nose configurations. The C_p distributions refer to stall conditions. All relevant aerodynamic coefficients for this case are summarized in Table 1.

3 Numerical approach

The present investigations are based on 2D simulations of the DLR F15 airfoil in high-lift configuration (Fig. 2). The CFD solver employed to perform the analysis is the DLR TAU-Code [23, 24], which uses a finite-volume approach for the solution of the Reynolds Averaged Navier–Stokes (RANS) equations. For the present study, a central scheme for the spatial discretization of the mean flow inviscid flux and a second order upwind Roe scheme for the convective turbulent flux were used. The turbulence model is given by Spalart and Allmaras with a correction due to flow rotation and curvature [25]. This last module enables the one-equation turbulence model to maintain a good accuracy in regions where the streamlines have a high curvature. This characteristic is fundamental for the simulation of the Coanda phenomenon, which is based on the equilibrium between the inertia forces and the momentum transport in the direction normal to the convex surface [18, 26]. This numerical set-up was validated by wind tunnel experiments [27]. In particular, the 3D flow simulations that included the wind tunnel wall effects were in good agreement with the experimental results [28].

The number of grid points was determined during previous studies [19], which did not include the suction slot. The mesh convergence exercise was based on the Richardson extrapolation [29]. This procedure provides an estimation of the spatial discretization error and of the minimum number of points that ensures an acceptable accuracy. Three grids were tested with the baseline

Table 1 Aerodynamic comparison between the clean nose and the flexible droop nose configurations $C_{\mu} = 0.06$

	$C_{l,max}$	α_{max} (°)	$C_{d,stall}$	$C_{m,stall}$
Clean nose	5.27	1.5	0.0886	-2.184
Droop nose	6.30	15.0	0.107	-2.44
Relative variation	+19.5 %	+13.5	+20.8 %	-11.7 %

configuration (clean nose but flap deflected and blowing slot), which contained around 70,000, 230,000 and 920,000 points. The corresponding maximum lift coefficients of 4.410, 4.456 and 4.480 were obtained for all the grids at $\alpha = 3.0^\circ$. Based on these values, the Richardson extrapolation yielded a value of the maximum lift coefficient of 4.496, which is an approximation of the $C_{l,max}$ that would be obtained using an infinite large number of grid points. This value is used as a reference value to determine the grid resolution error, which is 1.91, 0.89 and 0.36 % for the three grids, respectively. The chosen grid is the medium one, since it represents a compromise between accuracy and computational cost.

For the present analyses the medium grid was modified to include the suction slot. It contains about 250,000 points and includes an unstructured region and a structured one. The structured grid layer starts from the surfaces and is extended to cover the region where the main viscous phenomena occur. It ensures y^+ lower than 1 near the wall. The grid plots of Figs. 7, 8 and 9 show some of the main features of the mesh. An important characteristic of the grid, that makes it suitable for high-lift simulations, is the density of points along the pressure side, as the stagnation point will be situated in this region and can move quite far from the leading edge for high angles of attack. A large number of points is therefore necessary to properly capture the flow attachment. The structured region is extended over a large area above the flap, to accurately capture vortices expected in case of flow separation from the flap. The flap trailing edge and the edges of both slot lips are discretized

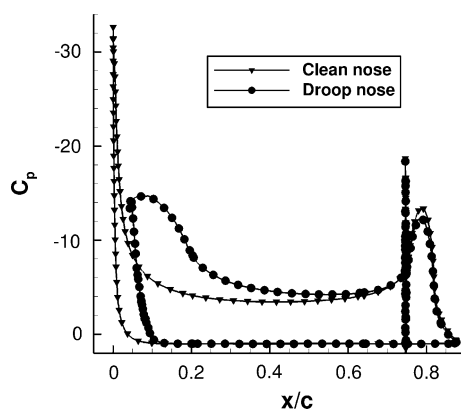


Fig. 6 C_p distributions at stall conditions, $C_{\mu} = 0.06$

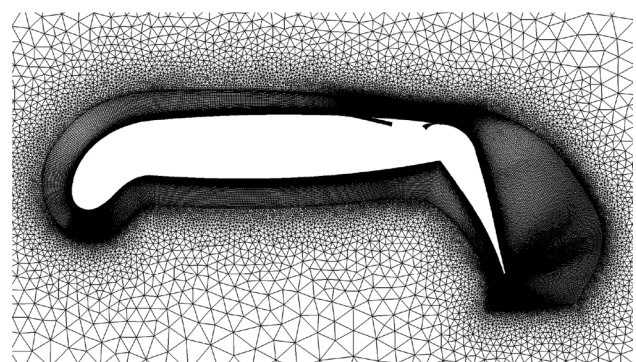


Fig. 7 Grid around the whole airfoil

by means of a local C-block topology (Fig. 8), to avoid the propagation of high point density into areas where grid points are not needed and could slow the convergence down.

4 Sensitivity study

In this section, the effects of shape and location of the suction slot are investigated. The sensitivity study draws an evaluation of the wall suction effect on both the maximum lift coefficient and the total pressure recovery inside the duct. This last quantity is fundamental for the design of the compact compressors, situated downstream of the wingbox, as shown in Fig. 1.

Previous analyses, performed with the configuration without suction, drew a clear picture in terms of jet momentum requirements and flow dynamics around the airfoil [19]. For the investigation presented in this section, the momentum coefficient was held constant at $C_{\mu} = 0.0356$. This particular momentum coefficient was chosen due to its sensitivity to the flow conditions upstream of the flap. With this blowing rate the jet has just the momentum required to avoid flow separation from the flap at maximum lift condition. A reduction in the required jet momentum would bring an increase of both the maximum lift and the stall angle of attack.

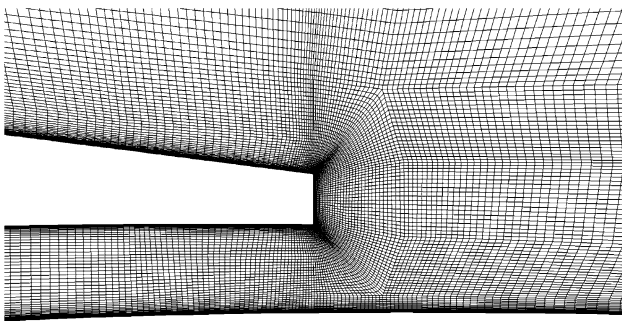


Fig. 8 Close-up of the grid at the blowing slot

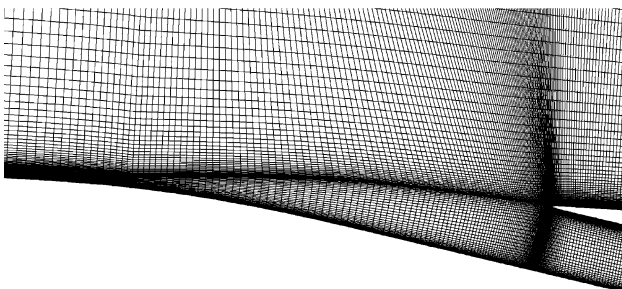


Fig. 9 Close-up of the grid at the suction slot

The mass flow through the suction slot was determined by the mass flow of the Coanda jet, fixed by the chosen C_{μ} . This value was then used to estimate the width at the end of the suction duct required to obtain a Mach number suited to represent the compressor inlet condition. For this purpose $M_{\text{inlet}} = 0.1$ was used, which, for a suction slot located at 61 % of the airfoil chord, resulted in a duct width of about 0.6 % of the chord length. The freestream conditions employed in the present work were $Re = 12 \times 10^6$ and $M = 0.15$.

Figure 10 shows the suction slot geometrical parameters that were varied in the present analysis. The sensitivity study is divided into two parts: analysis of the internal shape of the duct (β and γ) and study of the suction location (x), which are presented in Sects 4.1 and 4.2, respectively. In order to compare the overall performance of the tested geometries, the two criteria presented above (maximum lift coefficient and total pressure recovery in the duct) are combined into a single parameter, a balanced lift coefficient, as detailed in Sect. 4.3.

4.1 Internal shape analysis

For the analysis presented in this section, the parameters β and γ , defining the internal shape of the suction duct, were varied, while the suction location x was fixed at 61 % of the airfoil chord. This location would correspond to the front edge of a hypothetical spoiler and it is downstream of the wingbox (see Fig. 1). Positioning the suction slot in the front of the wingbox would involve the duct to pass through the supporting structure of the wing. Minimum value for the angle β was 10° . Lower angles may have yielded slightly better pressure recovery inside the duct but they would have also led to additional structural challenges, since a thinner lip would deform more when exposed to the pressure difference between the internal and the external flow.

Figure 12 shows the effect of the diffuser angle γ on the lift curve, for a fixed duct angle $\beta = 10^\circ$ (Fig. 11). The effect of the wall suction results in an increase of maximum lift coefficient of about 7 %, for the highest diffusion, $\gamma = 7^\circ$, and of 3° for the corresponding angle of attack. The increase of diffuser angle slightly improves the maximum lift coefficient without having a significant effect on

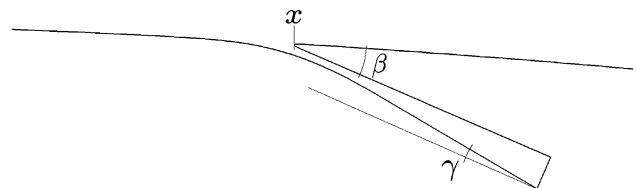


Fig. 10 Suction slot geometrical parameters

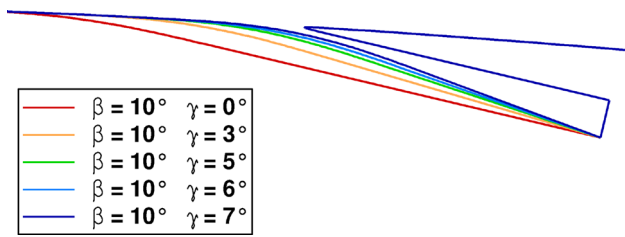


Fig. 11 Diffuser angle variations for $\beta = 10^\circ$

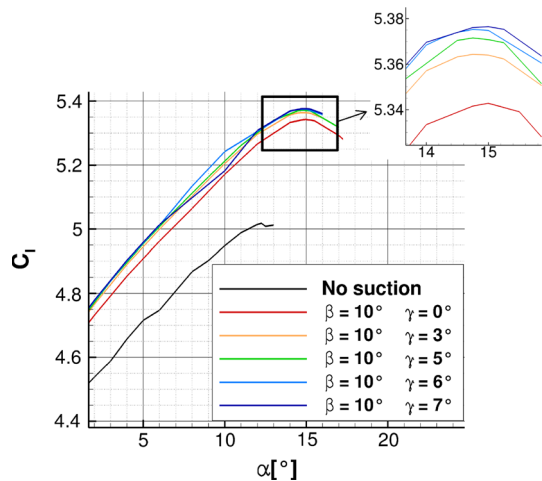


Fig. 12 Effect of diffuser angle on maximum lift performance, for $\beta = 10^\circ$, $Re = 12 \times 10^6$, $M = 0.15$

the stall angle of attack. The lift coefficient increase is about 0.6 %, for a variation of γ from 0° to 7° . Similar variations are obtained by setting the duct angle $\beta = 20^\circ$, where C_l is improved from 5.354 to 5.373 with γ varying from 0° to 7° . The influence of the different internal geometries on the total pressure recovery is described in Sect. 4.3, and reported in Table 4.

4.2 Location analysis

Having assessed the potential of the wall suction at 61 % chord length, the suction slot location with fixed $\beta = 10^\circ$ and $\gamma = 0^\circ$ was then varied to 30, 85 and 75 % chord on the pressure side, as illustrated in Figs. 13, 14 and 15, respectively. The three suction slot locations were selected based on their widely different effect on the flow physics. At 30 % chord length, the flow experiences an adverse pressure gradient after the peak around the leading-edge region. This pressure gradient increases the boundary layer thickness along the suction side of the airfoil, reducing the efficiency of the Coanda flap. For this reason, an improvement of the boundary layer in this area may significantly reduce the required jet momentum coefficient. At

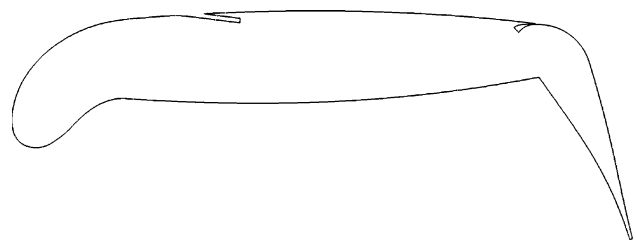


Fig. 13 Airfoil equipped with wall suction at 30 % chord length

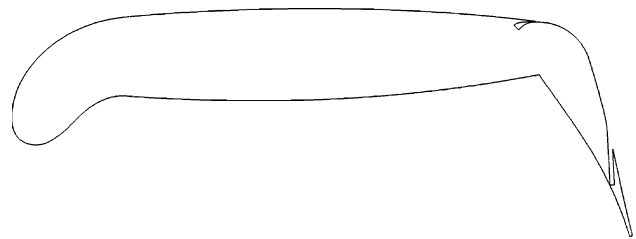


Fig. 14 Airfoil equipped with wall suction at 85 % chord length

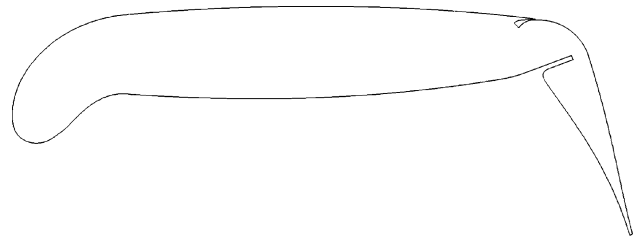


Fig. 15 Airfoil equipped with wall suction at 75 % chord length on the pressure side

85 % chord length the suction slot is located on the flap surface. In this location it may be possible to avoid the flow separation that occurs with low jet momentum coefficients, exploiting a mechanism similar to the one described by Chen [12]. Finally, a suction slot was located on the pressure side, at 75 % chord length, to reduce the recirculation area at the flap hinge and benefit from the high static pressure present in this area.

Figure 16 illustrates the lift curves of the different configurations. The location of the suction slot appears to have a higher influence on the aerodynamic performances compared to variations of the internal shape. With suction at 30 % chord, C_l is improved by about 12 % and the stall angle of attack is increased by 6° , with respect to the case without suction. On the other hand, the 85 % location decreases the maximum lift coefficient by 0.7 % and the angle of maximum lift by 1° . Locating the suction slot near the flap hinge does not have a significant effect on the lift performance. Details about the flow dynamics for the different suction locations are presented in the following sections.

4.2.1 Suction upstream of the Coanda jet

Considering the performance improvement shown in Fig. 16, it is worthwhile to investigate in more detail the effect of wall suction upstream of the blowing slot. Both the slot at 30 % chord and at 61 % chord improve the lift performance by increasing the momentum of the near-wall flow that has to be kept attached to the flap. Figure 17 shows the velocity profiles of the boundary layer just upstream of the blowing slot. It becomes evident that the momentum of the flow in the case of suction at 30 % chord is higher than the other cases. The boundary layer momentum thickness values at the same location, reported in Table 2, confirm this trend.

The lower momentum loss of the boundary layer in the 30 % chord case yields an overall increase of circulation around the airfoil, and a higher flow velocity around the leading edge. These improvements can be observed through Fig. 18, which reports the pressure coefficient distributions for the two suction locations upstream of the

Coanda jet and for the airfoil without suction. The effect of the suction on the pressure distribution appears similar to an increase of jet momentum coefficient, enabling a reduction of C_{μ} required to reach a certain lift coefficient, as detailed in Sect. 5.2.

4.2.2 Suction on the flap surface

The aerodynamic performance comparison presented in Fig. 16 is obtained with $C_{\mu} = 0.0356$, which enables the flow to follow the contour of the flap without separation. Under these conditions, a slot positioned on the flap surface removes part of the Coanda jet, reducing the momentum of

Table 2 Boundary layer momentum thickness upstream of the blowing slot $C_{\mu} = 0.0356$, $\alpha = 10^\circ$, $Re = 12 \times 10^6$, $M = 0.15$

	No suction	61 % c	30 % c
δ_2/c	1.29912e-03	9.75340e-04	7.82365e-04

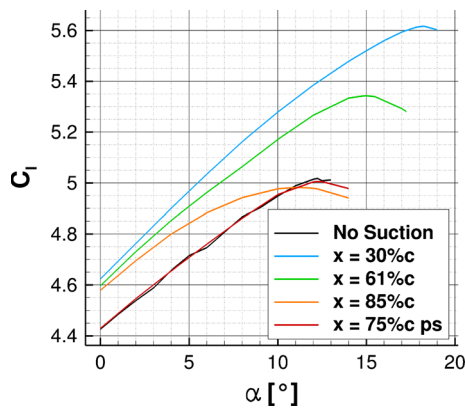


Fig. 16 Effect of suction location, $C_{\mu} = 0.0356$, $Re = 12 \times 10^6$, $M = 0.15$

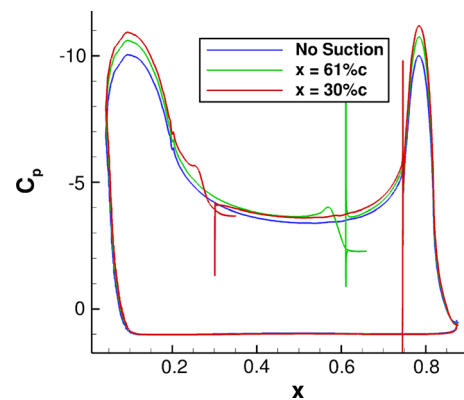


Fig. 18 C_p distributions for $C_{\mu} = 0.0356$, $\alpha = 10^\circ$, $Re = 12 \times 10^6$, $M = 0.15$

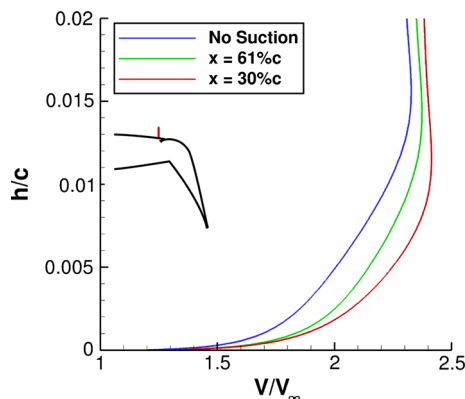


Fig. 17 Velocity profiles of the boundary layer upstream of the blowing slot, $C_{\mu} = 0.0356$, $\alpha = 10^\circ$, $Re = 12 \times 10^6$, $M = 0.15$

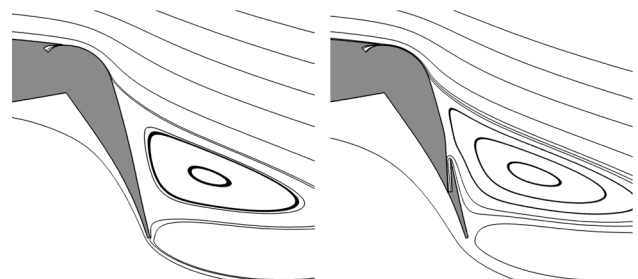


Fig. 19 Effect of wall suction at 85 % c on the flow over the flap, $C_{\mu} = 0.016$, $\alpha = 10^\circ$, $Re = 12 \times 10^6$, $M = 0.15$, left without suction, right with suction

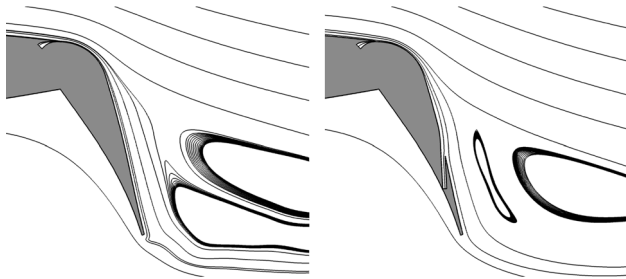


Fig. 20 Effect of wall suction at 85 % c on the flow over the flap at maximum lift condition, (without suction at 17° , left, and with suction at 15.25° , right), $C_\mu = 0.016$, $Re = 12 \times 10^6$, $M = 0.15$

the flow over the flap. This suction location might therefore be more effective for lower jet momentum coefficients. For this reason additional computations were conducted with $C_\mu = 0.016$. Now, the jet does not have sufficient momentum to keep the outer flow attached until the trailing edge. Figure 19 illustrates the flow field over the flap for angles of attack within the linear range of the lift curve. At these conditions, the suction mass flow seems to be not sufficient to avoid separation. A solution could be moving the suction slot closer to the separation point. However, at maximum lift conditions (17° without suction and 15.25° with suction) the separation occurs between the outer flow and the wall jet, which remains attached to the flap making wall suction ineffective (Fig. 20). This flow behavior is reflected in the maximum lift coefficients and the corresponding angles of attack, as summarized in Table 3. Details about the stall behavior of the Coanda flap without suction are described by Burnazzi and Radespiel in Ref. [22].

4.2.3 Suction at the flap hinge

The corner on the pressure side of the airfoil, created by the flap deflection, causes a recirculation area that might adversely affect the lift coefficient. Moreover, this area is characterized by a high static pressure. For these reasons the wall suction in this location may be beneficial for both the lift coefficient and the pressure recovery inside the duct. As illustrated in Fig. 21, the suction completely removes the recirculation structure from the flap hinge, and the total pressure obtained from the suction at this location is higher than the previous cases, as discussed in Sect. 4.3.

4.3 C_l balance

As previously mentioned, the objectives of the wall suction are (1) to provide air with high pressure recovery to the compact compressors, and (2) to improve the maximum lift generated by the airfoil. Unfortunately, these two objectives follow opposite trends when the geometrical

Table 3 Effect of suction at 85 % of the chord length, $C_\mu = 0.016$, $Re = 12 \times 10^6$, $M = 0.15$

	$C_{l,max}$	α_{stall} ($^\circ$)
No suction	3.877	17
Suction at 85 % c	3.82	15.25

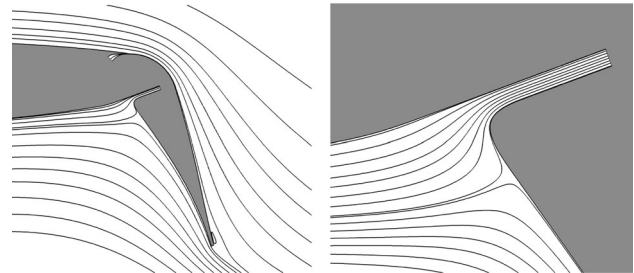


Fig. 21 Streamlines for the wall suction at the flap hinge, $C_\mu = 0.0356$, $\alpha = 10^\circ$, $Re = 12 \times 10^6$, $M = 0.15$

parameters are varied; a narrow suction slot would increase lift but would also induce higher viscous losses to the internal flow, reducing the suction pressure recovery. For this reason, a combined quantity is needed to compare the overall performance of the tested geometries. The approach proposed here is based on the following considerations:

- The total pressure at the end of the suction slot is an important parameter for the operation of the compact compressor; with a higher inlet total pressure, the compressor would need less power to provide the outlet total pressure needed by the Coanda jet. Similarly, for a given compression ratio, the compressor would provide a higher outlet total pressure.
- A higher total pressure inside the jet plenum (compressor outlet) would provide a higher C_μ .
- The lift coefficient is approximately directly proportional to the C_μ , for small variations of C_μ .

Therefore, it can be deduced that a higher suction pressure recovery would lead to a higher lift coefficient, for a given compression ratio. Thanks to this relation, it is possible to balance the lift coefficient with the total pressure obtained at the end of the suction slot.

Figure 22 illustrates the procedure to obtain the balanced lift coefficient. The first step is the computation of a new total pressure inside the jet plenum (outlet of the compact compressor), which is obtained by multiplying the total pressure at the end of the suction duct by a reference compression ratio. A new jet momentum coefficient is then obtained using the shape of the blowing slot and the outlet conditions. Subsequently, the new jet momentum coefficient is compared to the initial one, employed to compute the flow solution. The difference of the two jet momentum

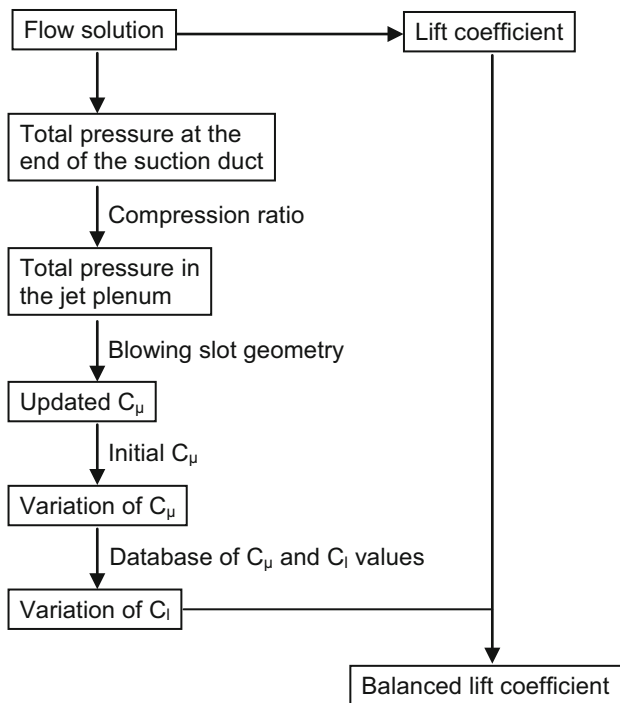


Fig. 22 Procedure to compute the balanced lift coefficient

coefficients is then used to estimate a variation of lift coefficient by means of a database containing C_{μ} and C_l values. Thanks to the lift coefficient variation, it is finally possible to compute the balanced lift coefficient.

This procedure does not take into account that a different jet would also induce variations to the suction flow. However, this effect would be rather small and it would simply increase the differences in the balanced performance shown here; a higher jet momentum would increase the airfoil circulation, thus the total pressure in the suction duct. In the following, the balance procedure is applied to the different test cases. The compression ratio was obtained by the total pressure inside the jet plenum and the one at the end of the suction slot for the geometry with $\beta = 10^\circ$, $\gamma = 0^\circ$, and $x = 61\%$ chord, used as a reference. For this reason, the balanced lift coefficient corresponding to this geometry does not differ from the initial one.

The balanced lift coefficient as a result of the internal shape analysis is presented in Fig. 23 and summarized in Table 4. The effect of the balance becomes more important for high diffusion angles, since the total pressure recovery is affected by the strong adverse pressure gradient along the duct. These cases present a lower total pressure at the end of the duct, which reduces the balanced jet momentum coefficient. As the figure shows, the most effective configuration with the highest balanced lift coefficient is obtained with $\beta = 10^\circ$ and $\gamma = 3^\circ$, for the $x = 61\%$ chord case.

Following the same procedure, the best suction slot location was also investigated. The analysis results are

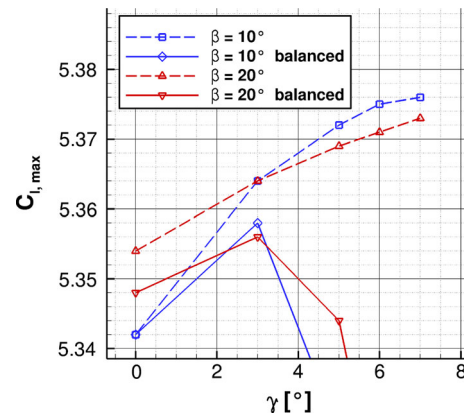


Fig. 23 Balanced performances from the internal shape analysis

Table 4 Balance for the internal geometries, with $x = 61\%$ c

	$C_{l,max}$	P_{ti}/P_∞	$C_{\mu,bal}$	$C_{l,max,bal}$
$\beta = 10^\circ, \gamma = 0^\circ$	5.342	0.9664	0.0356	5.342
$\beta = 10^\circ, \gamma = 3^\circ$	5.364	0.9652	0.0355	5.358
$\beta = 10^\circ, \gamma = 5^\circ$	5.372	0.9578	0.0349	5.328
$\beta = 10^\circ, \gamma = 6^\circ$	5.375	0.9348	0.0328	5.214
$\beta = 10^\circ, \gamma = 7^\circ$	5.376	0.8548	0.0257	4.735
$\beta = 20^\circ, \gamma = 0^\circ$	5.354	0.9652	0.0355	5.348
$\beta = 20^\circ, \gamma = 3^\circ$	5.364	0.9649	0.0355	5.356
$\beta = 20^\circ, \gamma = 5^\circ$	5.369	0.9615	0.0351	5.344
$\beta = 20^\circ, \gamma = 6^\circ$	5.371	0.9556	0.0346	5.316
$\beta = 20^\circ, \gamma = 7^\circ$	5.373	0.9371	0.0330	5.224

presented in Fig. 24 and Table 5. The highest total pressure is achieved at the end of the duct positioned at 75 % chord on the pressure side (ps), thanks to the high static pressure in this area. However, even translating this higher duct pressure into a higher jet momentum, the lift coefficient remains lower than the one achieved by the two locations upstream of the suction slot. The most effective location is 30 % of the chord length, although the pressure recovery is lower than for the other cases. Figure 24 shows the effect of the balance, which reduces significantly the differences in $C_{l,max}$ without changing the trend.

5 Performance evaluation

5.1 Response to C_{μ} variations

The geometry characterized by $\beta = 10^\circ, \gamma = 0^\circ, x = 61\%$ chord was tested with different jet momentum coefficients, and compared with results previously obtained without suction. The effect of the same suction device was also investigated on the clean nose configuration. Figures 25

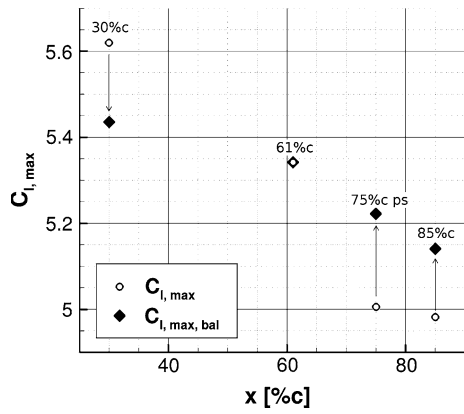


Fig. 24 Balanced performances for the location analysis

Table 5 Balance for the locations, with $\beta = 10^\circ$ and $\gamma = 0^\circ$

	$C_{l,max}$	P_{it}/P_∞	$C_{\mu,bal}$	$C_{l,max,bal}$
$x = 30 \% c$	5.620	0.9302	0.0324	5.435
$x = 61 \% c$	5.342	0.9664	0.0356	5.342
$x = 85 \% c$	4.982	1.0016	0.0387	5.141
$x = 75 \% c$ ps	5.006	1.0154	0.0397	5.222

and 26 show the effects of C_μ on the stall angle of attack and the maximum lift coefficient. On both parameters the effect of wall suction appears to be larger in presence of the droop nose device. With $C_\mu = 0.0356$, α_{stall} increases by 2.75° , for the droop nose configuration, and only 0.5° for the clean nose geometry (Fig. 25). For the same jet momentum coefficient, the maximum lift coefficient for the droop nose configuration is increased by about 6.5 % due to suction, whereas for the clean nose configuration the increase is only 3 % (Fig. 26). These differences are similarly observed in the entire range of C_μ tested here. Furthermore, the curves corresponding to the same leading-

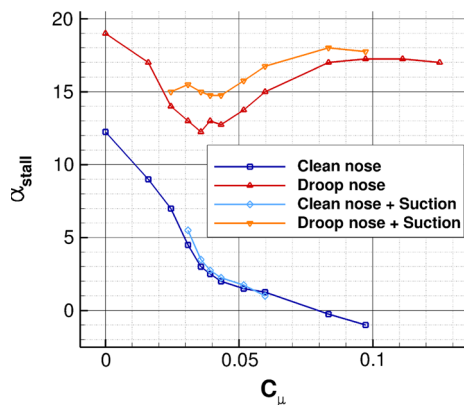


Fig. 25 Effect of C_μ on the stall angle of attack, $Re = 12 \times 10^6$, $M = 0.15$

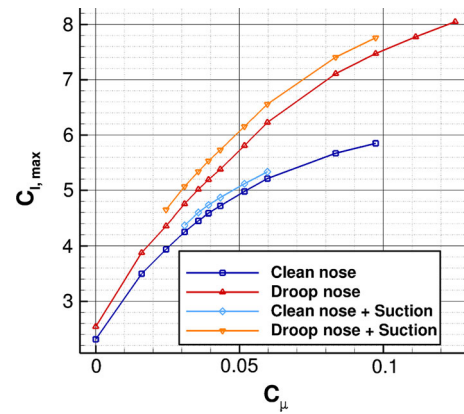


Fig. 26 Effect of C_μ on the maximum lift coefficient, $Re = 12 \times 10^6$, $M = 0.15$

Table 6 Blowing requirement and aerodynamic parameters corresponding to $C_l = 5$

	C_μ	α ($^\circ$)	C_l	C_m
Baseline	0.0522	1.5	5.0	-0.880
Droop nose	0.0353	12.3	5.0	-0.724
Droop nose + suction	0.0298	15.4	5.0	-0.641

edge configuration on Figs. 25 and 26 follow a similar trend, which means that the stall mechanisms are not significantly affected by the suction device.

5.2 Efficiency for a fixed lift coefficient

Table 6 shows the large improvements achieved by the leading-edge device and wall suction. The suction slot configuration chosen for this comparison is the one used as reference for the previous analyses: $\beta = 10^\circ$, $\gamma = 0^\circ$, $x = 61 \%$ chord. The benefit of the droop nose device and the wall suction is to reduce the required blowing power, and to increase the angle of attack of maximum lift coefficient. As shown in Table 6, a target $C_l = 5.0$ can be obtained with about 32 % less jet momentum thanks to the droop nose, which becomes about 43 % if the wall suction is also implemented. As a consequence, a lift gain factor of 105 is obtained, to be compared with the value provided by the baseline configuration, 60, and by the same geometry without suction, 89. Note that the stall angle in this lift range is brought to values suitable for landing and takeoff operations: from 1.5° to 12.3° for the droop nose and to 15.4° for both droop nose and suction. The pitching moment represents an important issue for the stability of the aircraft, and due to an improved load distribution along the chord, and the lower jet momentum requirement, the pitching moment is improved by about 18 % by the droop nose and 27 % including also the effect of the suction.

6 Conclusions

The present work reports on the progress of new active high-lift technologies. The analyzed active high-lift configuration consisted of a Coanda flap, and a suction slot. The study focused on the aerodynamic sensitivities of the suction slot geometry and location. The interaction between the two active flow control principles, tangential blowing and wall suction, was also investigated yielding physical insight into the flow mechanisms.

The objectives of the sensitivity study were the total pressure recovery along the suction duct and the lift coefficient. The analysis of the suction duct internal shape showed that a narrower slot induces higher lift, but also higher viscous losses inside the duct, reducing the total pressure recovery. For this reason, the two objectives were combined into one single quantity, a balanced lift coefficient, employed to compare the overall performance of the different test cases. The results highlight the high efficiency of suction on the suction side of the airfoil upstream of the Coanda flap. In these cases, the airfoil generated a higher lift than with suction on the flap surface or on the pressure side, showing that better performances are achieved by exploiting the synergies between the two flow control devices. In particular, the highest lift was obtained by locating the suction slot at 30 % chord, which is just downstream of the low pressure peak at the leading edge. This leads to a reduction of the boundary layer momentum thickness upstream of the blowing slot, which reduces the jet momentum required to avoid flow separation from the flap. Using suction on the flap surface to avoid flow separation in presence of low jet momentum showed to be ineffective due to the complex flow topology over the flap. Until a few degrees before stall, the wall suction was not sufficient to remove the separation. At stall conditions, the recirculation area occurs between the outer flow and jet, which remains attached to the flap surface making wall suction not effective. The suction slot was also tested near the flap hinge, which is an area of high static pressure. The total pressure at the end of the suction duct was higher than for the other suction locations, but the effect of suction on the lift coefficient was significantly lower.

Finally, the maximum lift performance of the airfoil with wall suction at 61 % chord was computed for different jet momentum coefficients. The suction yielded a significant reduction of the blowing momentum requirements and increased the angle of attack of maximum lift. The target $C_1 = 5.0$ could be achieved with 16 % less blowing momentum, with respect to the same configuration without suction, and the maximum angle of attack was increased from 12.3° to 15.4° . Consequently, the lift gain factor was increased from 89 to 105. Moreover, wall suction was found to be about twice as effective when applied in

presence of a droop nose leading-edge device, rather than the clean nose configuration.

In the future the expertise gained during the present work will be employed to design a 3D model of the suction slot that will lead air to the compact compressors. In this context, 3D computations will take into account other constraints due to 3D geometry requirements.

Acknowledgments The funding of this work of the Collaborative Research Centre SFB 880 by the German Research Foundation, DFG, is thankfully acknowledged.

References

- Prandtl, L.: The generation of vortices in fluids of small viscosity. Aeronautical Reprints, The Royal Aeronautical Society No. 20, London (1927)
- Teichel S., et.al.: Optimized preliminary design of compact axial, compressors. In: A comparison of two design tools 31st AIAA Applied Aerodynamics Conference, San Diego (2013)
- NASA: Aeronautics Research Strategic Vision, A blueprint for transforming global air mobility. http://www.aeronautics.nasa.gov/pdf/armd_strategic_vision_2013.pdf (2013)
- Pott-Pollenske, M., Alvarez-Gonzalez, J., Dobrzynski, W.: Effect of slat gap on farfield radiated noise and correlation with local flow characteristic. In: 9th AIAA/CEAS Aeroacoustics Conference, Hilton Head AIAA (2003)
- Werner-Spatz, C., Heinze, W., Horst, P., Radespiel, R.: Multi-disciplinary conceptual design for aircraft with circulation control high-lift systems. CEAS. Aeronaut. J. **3**, 145–164 (2012)
- Wynanski, I.: The variables affecting the control of separation by periodic excitation. In: 2nd AIAA Flow Control Conference. AIAA, Portland. 2505 (2004)
- Gad-El-Hak, M.: Flow control: passive, active, and reactive flow management. Cambridge University Press, London (2000)
- Englar, R.J.: Overview of circulation control pneumatic aerodynamics: blown force and moment augmentation and modification as applied primarily to fixed-wing aircraft. Appl. Circ. Control. Technol., Prog. Astronaut. Aeronaut., AIAA **214**, 23–68 (2006)
- Milholen, W., Jones, G., Chan, D.: High-reynolds number circulation control testing in the national transonic facility (invited). In: 50th AIAA Aerospace Sciences Meeting. AIAA, 0103 (2012)
- Schlichting, H.: Boundary-layer theory. Mc-Graw Hill Publications, New York (1960)
- Loftin, J.K., Burrows, D.L.: Investigations relating to the extension of laminar flow by means of boundary layer suction through slot, NACA report (1961)
- Chen, C., Seele, R., Wynanski, I.: Flow Control on a Thick Airfoil Using Suction Compared to Blowing. AIAA. J. **51**(6), 1462–1472 (2013)
- Allan, B., Jones, G., Lin, J.: Reynolds-Averaged Navier-Stokes simulation of a 2D circulation control wind tunnel experiment. In: 49th AIAA Aerospace Sciences Meeting, pp. 25. AIAA, Orlando (2011)
- Paschal, K., Neuhart, D., Beeler, G., Allan, B.: Circulation control model experimental database for CFD validation. In: 50th AIAA Aerospace Sciences Meeting, vol. 0705. AIAA, Nashville (2012)
- Radespiel, R., Pfingsten, K.-C., Jensch, C.: Flow analysis of augmented high-lift systems. In: Radespiel, R., Rossow, C.-C., Brinkmann, B. (eds) Hermann Schlichting—100 Years. Scientific Colloquium Celebrating the Anniversary of his Birthday,

- Braunschweig, Germany 2007. Notes on Numerical Fluid Mechanics and Multidisciplinary Design, vol. 102. Springer, New York (2009). ISBN:978-3-540-95997-7
16. Jensch, C., Pflingsten, K.C., Radespiel, R., Schuermann, M., Haupt, M., Bauss, S.: Design aspects of a gapless high-lift system with active blowing, DLRK Aachen (2009)
 17. Jensch, C., Pflingsten, K.C., Radespiel, R.: Numerical investigation of leading edge blowing and optimization of the slot and flap geometry for a circulation control airfoil, notes on numerical fluid mechanics and multidisciplinary design, vol. 112. Springer, Berlin (2010)
 18. Pflingsten, K.C., Jensch, C., Körber, K.V., Radespiel, R.: Numerical simulation of the flow around circulation control airfoils. In: First CEAS European Air and Space Conference, Berlin (2007)
 19. Burnazzi, M., Radespiel, R.: Design and analysis of a droop nose for coanda flap applications. *J. Aircr.* **51**(5), 1567–1579 (2014). doi:[10.2514/1.C032434](https://doi.org/10.2514/1.C032434)
 20. Wild, J.: Experimental investigation of Mach- and Reynolds-number dependencies of the stall behavior of 2-element and 3-element high-lift wing sections. In: 50th AIAA Aerospace Sciences Meeting, vol. 108. AIAA, Nashville (2012)
 21. Englar, R.J., Smith, M.J., Kelley, S.M., Rover, R.C.: Application of circulation control to advanced subsonic transport aircraft, Part I: airfoil development. *J. Aircraft.* **31**(5), 1160–1168 (1994)
 22. Burnazzi, M., Radespiel, R.: Assessment of leading-edge devices for stall delay on an airfoil with active circulation control. *CEAS Aeronaut. J.* **5**(4), 359–385 (2014). doi:[10.1007/s13272-014-0112-5](https://doi.org/10.1007/s13272-014-0112-5)
 23. Kroll, N., Rossow, C.-C., Schwaborn, D., Becker, K., Heller, G.: MEGAFLOW—a numerical flow simulation tool for transport aircraft design. ICAS Congress, Toronto (2002)
 24. Schwaborn, D., Gerhold, T., Heinrich, R.: The DLR TAU-Code: recent applications in research and industry. ECCOMAS CFD, Egmond aan Zee, The Netherlands (2006)
 25. Shur, M.L., Strelets, M.K., Travin, A.K., Spalart, P.R.: Turbulence modeling in rotating and curved channels: assessing the spalart-shur correction. *AIAA. J.* **38**, 784–792 (2000)
 26. Swanson, R.C., Rumsey, C.L.: Computation of circulation control airfoil flows. *Comput. Fluids.* **38**, 1925–1942 (2009)
 27. Pflingsten, K.C., Cecora, R.D., Radespiel, R.: An experimental investigation of a gapless high-lift system using circulation control. Katnet II Conference, Bremen (2009)
 28. Pflingsten, K.C., and Radespiel, R.: Experimental and numerical investigation of a circulation control airfoil. In: 47th AIAA Aerospace Sciences Meeting, pp. 533. AIAA, Orlando (2009)
 29. Richardson, L.F.: The deferred approach to the limit. *Transactions of the Royal Society of London, Series A* **226**, 299–361 (1927)